Mechanism of Tianxiang Dan in Inhibiting Atherosclerosis Progression by Regulating the Autophagy-mTOR-AIM2 Inflammasome Axis Based on ApoE$^{-/-}$ and NLRP3$^{-/-}$ Mouse Models

Longlong GUO[1,2△], Yue DONG[2△], Li ZHANG[1,2], Longfei SUN[2], Xiaxia ZHANG[1], Lintao GUO[1], Wenijie WEI[1], Zhaoju WANG[2*], Dongqing AN[1,2*]

1. Xinjiang Medical University, Urumqi 830017, China; 2. Xinjiang Uygur Autonomous Region Hospital of Traditional Chinese Medicine, Urumqi 830000, China

Abstract [**Objectives**] To explore the effect of Tianxiang Dan in inhibiting the progression of atherosclerosis in mice by regulating the autophagy-mammalian target of rapamycin (mTOR)-absent in melanoma 2 (AIM2) inflammatoryosome axis and its mechanism. [**Methods**] Atherosclerosis models of ApoE knockout (ApoE$^{-/-}$) mice were established by feeding with a high-fat diet for 12 weeks. The mice were divided into the model group (MD group), Tianxian Dan group [2.73 g/(kg · d), TXD group], ApoE$^{-/-}$ · NACHT, LRR and PYD domain protein 3 (NLRP3)$^{-/-}$ + TXD group [2.73 g/(kg · d), NLRP3$^{-/-}$ group] and ApoE$^{-/-}$ · NLRP3$^{-/-}$ + RGFP966 group [400 μg/(kg · d), RGFP966 group], with 10 mice in each group. Ten C57BL/6J mice were fed with the basic diet as the blank control group (CO group). The plaque burden and stability were evaluated by oil red O staining, hematoxylin-eosin (HE) and Masson staining. The morphology of autophagosomes in aortic tissue was observed under transmission electron microscopy. The expressions of microtubule-associated protein 1 light chain 3 (LC3), myosinlike BCL2-binding protein (Beclin-1), phosphorylated mTOR (p-mTOR), AIM2, Caspase-1, pyroptosis factor D (GSDMD), interleukin-1β (IL-1β), and interleukin-18 (IL-18) proteins were detected by Western Blot. The mRNA expression of AIM2 was detected by immunohistochemistry and real-time fluorescence quantitative reverse transcription polymerase chain reaction (qRT-PCR). The levels of IL-1β and IL-18 in serum and aortic homogenate were determined by enzyme-linked immunosorbent assay (ELISA), and correlation analysis was performed. [**Results**] Compared with the MD group, the protein expressions of AIM2, p-mTOR, Caspase-1, GSDMD, IL-1β, IL-18, and the serum levels of IL-1β and IL-18, the mRNA expression AIM2 in the TXD group decreased, while the protein expressions of LC3 and Beclin-1 increased ($P<0.05$). Compared with the TXD group, the protein expressions of AIM2, p-mTOR, Caspase-1, GSDMD, and AIM2 mRNA in the NLRP3$^{-/-}$ group increased, while the protein expressions of IL-18, LC3, Beclin-1, and the serum content of IL-18 decreased ($P<0.05$). Compared with the TXD group, the protein expression and serum content of IL-18 in the RGFP966 group decreased ($P<0.05$). Correlation analysis showed that LC3 was negatively correlated with AIM2, GSDMD, IL-1β, IL-18, and p-mTOR was positively correlated with AIM2, GSDMD, IL-1β, and IL-18. [**Conclusions**] Tianxiang Dan could reduce plaque burden and enhance plaque stability, and its mechanism might be related to the regulation of the autophagy-mTOR-AIM2 inflammatory pathway.

Key words Atherosclerosis, Tianxian Dan, Autophagy-mammalian target of rapamycin-absent in melanoma 2 inflammatory pathway, Mice, Experimental study

1 Introduction

Atherosclerosis serves as a critical pathological foundation for cardiovascular events, with its development accompanied by lipid deposition in the vascular wall, immune cell infiltration, and persistent inflammatory responses[1]. Although lipid-modifying and antiplatelet aggregation therapies significantly reduce the incidence of cardiovascular events, residual inflammatory risks persist[2]. Therefore, it does not fully halt the progression of atherosclerosis by solely targeting blood lipids[3]. In recent years, inflammasome mediated programmed inflammatory pyroptosis has become an important mechanism connecting aseptic inflammation and plaque instability[4]. The role of the classical NOD-like receptor family Pyrin domain protein 3 (NLRP3) inflammasome in atherosclerosis has been reported[5]. Relevant research evidence suggests that it is difficult to fully explain the sustained increase of inflammatory factors in the vascular wall and the phenomenon of pyroptosis in multiple cell types solely from the perspective of NLRP3[6]. As an inflammasome receptor that recognizes intracellular double stranded deoxyribonucleic acid (DNA), absent in melanoma 2 (AIM2) can respond to signals such as mitochondrial DNA release, nuclear DNA damage, and apoptotic cell debris, playing an important role in various DNA driven inflammatory diseases[7]. Some studies suggest that AIM2 inflammasome may participate in the formation and progression of atherosclerotic plaques rich in apoptotic/necrotic cells and nucleic acid fragments[8]. Autophagy is a key degradation pathway that maintains cellular homeostasis, and inhibits inflammatory responses by clearing damaged mitochondria and protein aggregates[9].

Mammalian target protein of rapamycin (mTOR) is a classic negative regulator of autophagy, and its sustained activation can significantly inhibit autophagy flow[10]. Previous studies have shown that autophagy negatively regulates NLRP3 inflammasome activation by degrading inflammasome components, reducing mitochondrial DNA and reactive oxygen release. Some experiments also suggest that autophagy may affect the perception and assembly

Received: May 15, 2026 Accepted: July 6, 2026

Supported by the Natural Science Foundation Project of Xinjiang Uygur Autonomous Region (2024D01B01); the National Natural Science Foundation Project of China (82274480, 82060861); the Graduate Innovation Project in Xinjiang Uygur Autonomous Region (XJ2024G180).

△These authors contributed equally to this work.

Longlong GUO, associate chief physician, doctoral degree. Yue DONG, attending physician. *Corresponding author. Zhaoju WANG, chief physician, master's degree. Dongqing AN, chief physician, professor, doctoral degree.

of intracellular DNA by AIM2 inflammasomes[11]. However, in the context of atherosclerosis, whether the autophagy-mTOR pathway is involved in the regulation of the AIM2 inflammasome-gasdermin D (GSDMD) axis and the specific role of this pathway in the pyroptosis and plaque progression in the vascular wall still lacks systematic research. RGFP966, a selective inhibitor of histone deacetylase 3 (HDAC3), is an epigenetic regulation related inhibitor with selective inhibitory effects, exerting anti-inflammatory and tissue protective effects in various cardiovascular and neurological disease models[12]. It has been suggested that RGFP966 may play a role by regulating the transcription of inflammatory genes and the state of cell metabolism[13]. But whether it can target the autophagy-mTOR-inflammasome axis, especially the activation of AIM2 inflammasome in atherosclerosis, has not yet been clear. Previous studies mostly focused on NLRP3 inflammasome, and lacked systematic evaluation on the independent contribution of AIM2 mediated pyroptosis in atherosclerosis and its response to drug intervention. The apolipoprotein E gene knockout (ApoE$^{-/-}$) and NLRP3$^{-/-}$ mice high-fat diet induced atherosclerosis model was used in this paper. Combined with RGFP966 drug and Tianxiang Dan intervention, it aimed to clarify the role of AIM2 inflammasome in protein expression of GSDMD, caspase-1, interleukin-1β (IL-1β), and interleukin-18 (IL-18) in plaque formation, further clarify the regulation of autophagy-mTOR pathway on this mechanism, and evaluate the impact of Tianxiang Dan on these pathways and its anti atherosclerosis mechanism.

2 Materials and methods

2.1 Experimental animals The experimental animals used in this paper were mice of C57BL/6J background, including 15 C57BL/6J mice and 15 ApoE$^{-/-}$ mice, all purchased from Beijing Charles River Experimental Animal Technology Co., Ltd., with animal license number SCXK (Beijing) 2021-0006. Three pairs of homozygous ApoE$^{-/-}$ · NLRP3$^{-/-}$ double knockout mice were purchased from Wuhan Youdu Biotechnology Co., Ltd., with animal license number SCXK (E) 2021-0025. After 3 months of breeding, 52 male mice were bred, and 35 were selected for the experiment. All mice were male, 8 weeks old, with a body weight of (20 ± 2) g. They were raised in the Specific Pathogen Free (SPF) Animal Experimental Center of Xinjiang Medical University, with an ambient temperature of (22 ± 1) ℃, relative humidity of 60% to 75%, and a light-dark cycle of 12 h. Animals were free to feed and drink water, and the environmental humidity ranged from 25.0% to 32.8%. This study was approved by the Experimental Animal Ethics Committee of Xinjiang Medical University (Approval No.: XY2023-206).

2.2 Experimental reagents and instruments Tianxiang Dan granules (produced by Xinjiang Qikang Habo Pharmaceutical Co., Ltd., lot No.: ZO4000820, specification: 9 g per pack); RGFP966 (item No.: HYN0822, Med Chem Express Company); hematoxylin-eosin (HE) staining solution (item No.: BL-700B, Biosharp Company), Masson staining solution (item No.: G1340, Solarbio Company), oil red O staining solution (item No.: 1320-06-5, Sigma Company), AIM2, Caspase-1, GSDMD, glyceraldehyde-3-phosphate dehydrogenase (GAPDH) primary antibody (item No.: Ab204995, Ab138483, Ab219800, Ab181602, Abcam Company), IL-1β, IL-18 primary antibody (item No.: AF5103, AF5183, Affinity Biosciences Company), IL-1β, IL-18 enzyme-linked immunosorbent assay (ELISA) kit (item No.: YX-E2053, YX-11382, Shanghai Youxuan Biotechnology Co., Ltd.). Paraffin slicer (Finesse325, USA Thermo Company), electrophoresis analyzer and electroporation analyzer (Power Pac Basic type, Bio-rad Company), image analyzer (DMR + 0550 type, Germany Leica Company).

2.3 Methods

2.3.1 Establishment and grouping of atherosclerosis model. The atherosclerosis model was induced by high-fat diet. High-fat diet formula: 72.5% of basic feed, 10% of lard, 5% of egg yolk, 10% of analytical grade, 2% of cholesterol, 0.2% of pig bile salt, 0.2% of propylthiouracil tablets, 0.1% of 21 hydroxyvitamin. Mice were fed with a high-fat diet for 12 weeks. After 12 weeks, 5 mice were selected from C57BL/6J mice, ApoE$^{-/-}$ mice, and ApoE$^{-/-}$ · NLRP3$^{-/-}$ mice respectively to verify the success of modeling. After the model was established, the mice were divided into MD group (ApoE$^{-/-}$ + high - fat diet + equal volume of physiological saline gavage), ApoE$^{-/-}$ + TXD group (high-fat diet + 2.73 g/(kg · d) of Tianxiang Dan gavage, TXD group), ApoE$^{-/-}$ · NLRP3$^{-/-}$ + TXD group (ApoE$^{-/-}$ · NLRP3$^{-/-}$ + high-fat diet + 2.73 g/(kg · d) of Tianxiang Dan gavage, NLRP3$^{-/-}$ group), ApoE$^{-/-}$ · NLRP3$^{-/-}$ + RGFP966 group (ApoE$^{-/-}$ · NLRP3$^{-/-}$ + high-fat diet + 3 mg/(kg · d) of RGFP966 gavage, RGFP966 group) and CO group (basic feed feeding + equal volume of saline gavage), once daily for 12 weeks.

2.3.2 Processing and collection of animal specimens. At the end of the experiment, the mice were fasted for 12 h. Approximately 1 mL of blood was collected using the orbital blood collection method, and then centrifuged (3 500 r/min, 15 min) to separate the serum. The serum was stored in a -80 ℃ of freezer for later use. All mice were euthanized by cervical dislocation, and the aortic arch was dissected and fixed with 4% of paraformaldehyde for 6 h. After dehydration, transparency, and paraffin embedding, sections were cut for subsequent pathological analysis. The remaining tissue samples were frozen in liquid nitrogen at -80 ℃ for the detection of autophagy and inflammasome related pathway proteins.

2.3.3 Pathological morphology observation. Oil red O staining: a sample of the aorta was taken. After longitudinally cut, it was immersed in oil red O staining solution to stain at 37 ℃ for 60 min. 75% ethanol was used to differentiate it until the fatty plaque turned orange red or bright red. After the stained tissue was washed with distilled water, photos were taken, and the plaque area was analyzed.

HE/Masson staining: after aortic tissue was fixed with 10% of formaldehyde, it was embedded in paraffin and sliced. The color pictures by HE staining and Masson staining were observed by an optical microscope, and the plaque area, fibrous cap thickness, and necrotic nucleus area were evaluated.

2.3.4 Western Blot detection of autophagy-mTOR signal, AIM2 inflammasome, and apoptosis related molecular proteins expression. After the tissue sample was lysed, the protein concentration was determined by the bicinchoninic acid or 2,2-biquinoline-4,4-dicarboxylic acid method (BCA). The protein sample was subjected to sodium dodecyl sulfate polyacrylamide gel electrophoresis (SDS-PAGE), and the protein was transferred to the polyvinylidene fluoride (PVDF) membrane using the membrane transfer equipment. After membrane closure, corresponding primary antibodies including microtubule associated protein 1 light chain 3 (LC3), myosin-like BCL2-binding protein (Beclin-1), phosphorylated manmalian target of rapamycin (p-mTOR), AIM2, Caspase-1, GSDMD, IL-1β, IL-18 (1∶500) were added and incubated overnight at 4 ℃. After the secondary antibody was labeled, the chemiluminescence kit was used for color development. The image was obtained by the Bio-Rad gel imaging system, and the band gray value was analyzed by the Image J software.

2.3.5 Immunohistochemical detection of AIM2 expression. Immunohistochemical detection was performed using paraffin sections. After dewaxing, the slices were subjected to antigen repair using sodium citrate, followed by treatment with hydrogen peroxide (H_2O_2) to inactivate endogenous peroxidase. After blocking with goat serum, the corresponding primary antibody (AIM2) was incubated, followed by secondary antibody incubation and color development. Finally, counterstaining and sealing were performed. Five fields of view were randomly selected under the microscope, and Image J was used to analyze the expression level of the target protein.

2.3.6 Real-time fluorescence quantitative reverse transcription polymerase chain reaction (qRT-PCR) detection of AIM2 mRNA expression. Total RNA was extracted from mouse aortic tissue and isolated using the Trizol method. After cDNA synthesis, the expression level of AIM2 mRNA was analyzed by qRT-PCR using SYBR Green. Relative quantitative analysis was performed using GAPDH as an internal reference. AIM2 forward primer: 5′-AGACTCAGGAAGGAAGACAAG-3′, reverse primer: 5′-GATTCAACATCAACCACAACT-3′, primer length: 193 bp; GAPDH forward primer: 5′-GAGAGTGTTTCCTCGTCCCGTA-3′, reverse primer: 5′-CCTCACCCCATTTGATGTTAGT-3′, primer length: 290 bp.

2.3.7 ELISA detection of IL-1β and IL-18 levels in serum and aortic homogenate. ELISA kit was used to detect the levels of IL-1β and IL-18 in serum and aortic homogenate. All operations were carried out according to the kit instructions, and the results were analyzed using statistical software.

2.4 Statistical processing SPSS 26.0 statistical software was used for data analysis. Quantitative data that conformed to normal distribution and homogeneity of variance were expressed as mean ± standard deviation ($\bar{x} \pm s$). One-way ANOVA was used for comparison between multiple groups, and *LSD* was used for comparison between two groups; quantitative data that did not follow a normal distribution were analyzed using Dunnett's T_3 test. Spearman analysis was used for correlation analysis. The difference was statistically significant with $P<0.05$.

3 Results and analysis

3.1 Mouse plaque formation and AIM2 activation HE staining of mice in CO group showed that the aortic tissue structure was intact, the intima was smooth and flat, and there was no obvious lipid deposition or plaque formation on the vessel wall. Masson staining showed that collagen fibers were evenly distributed, and no obvious abnormalities were observed. Immunohistochemistry showed the intima was smooth, with visible light yellow positive staining. HE staining of mice in MD group showed structural damage to the aortic tissue, poor integrity of the intima, disordered arrangement of endothelial cells, lipid deposition on the vessel wall, thinning of the fibrous cap, and formation of plaques. Masson staining showed deposition of collagen fibers, which were unevenly distributed. Immunohistochemistry showed plaque formation with dark brownish yellow positive staining. The results were shown as Fig. 1. Compared with the CO group, the expression levels of AIM2, Caspase-1, GSDMD, IL-1β, and IL-18 in the aorta of the MD group were increased, and the differences were statistically significant ($P<0.05$). Compared with the CO group, AIM2 mRNA expression was upregulated, and the difference was statistically significant ($P<0.05$). Compared with the CO group, the expression levels of serum IL-1β and IL-18 increased in the MD group, and the differences were statistically significant ($P<0.05$). The results were shown as Fig. 2 – 3.

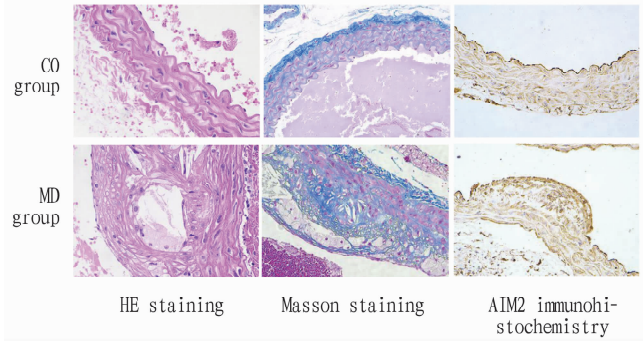


Fig. 1 Pathological changes in aortic tissue of two groups of mice (×400)

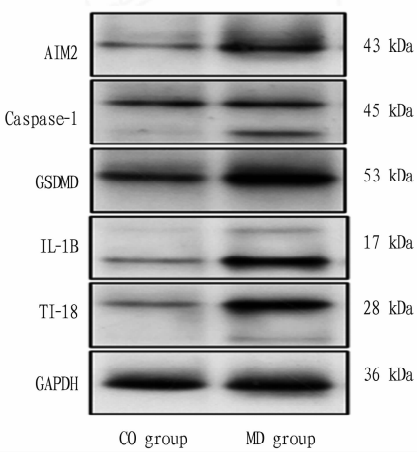
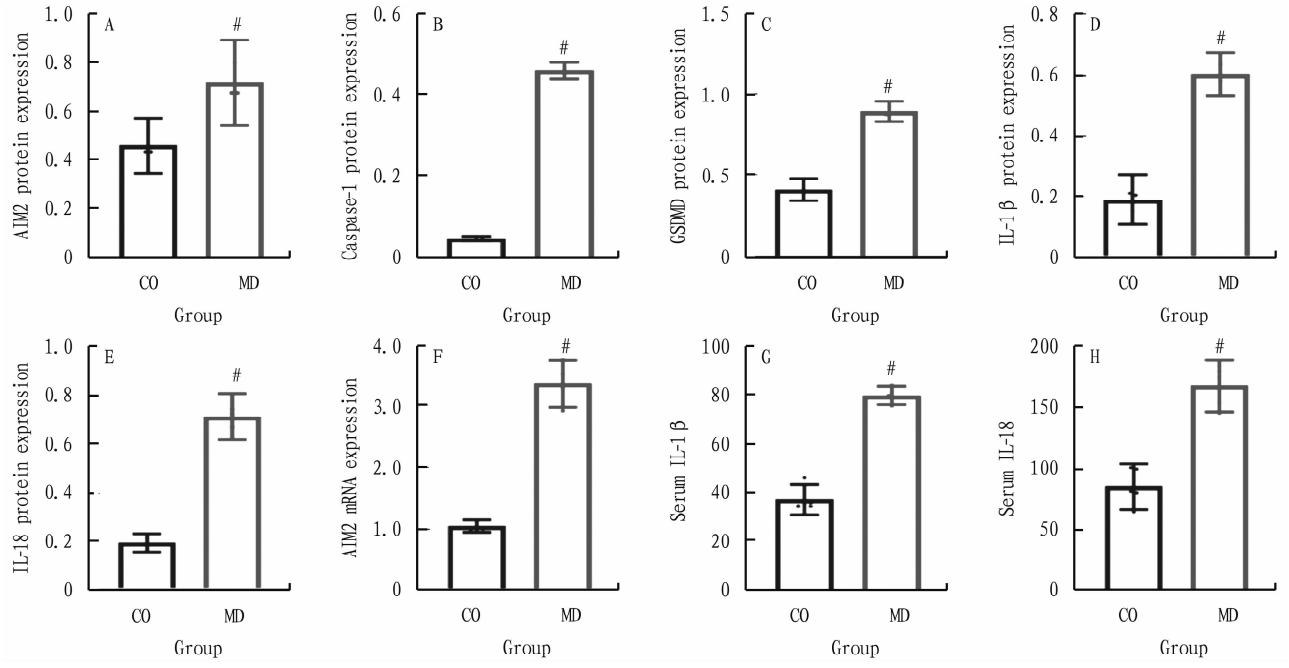


Fig. 2 Band diagram of AIM2 pathway related protein expression in aortic tissues of two groups of mice



NOTE A represents the changes in AIM2 protein; B represents the changes in Caspase-1 protein; C represents the changes in GSDMD protein; D represents the changes in IL-1β protein; E represents the changes in IL-18 protein; F represents the changes in AIM2 mRNA; G represents the changes in serum IL-1β; H represents the changes in serum IL-18 level. Compared with the CO group, # shows $P<0.05$.

Fig. 3 Comparison of AIM2 pathway related proteins, mRNA, and serum IL-1β and IL-18 levels in aortic tissues of two groups of mouse

3.2 Expression of autophagy pathway related proteins in aortic tissue of mouse Compared with the CO group, the expression of p-mTOR in the aortic tissue of mice in MD group increased, while the expression of Beclin-1 and LC3 proteins decreased, and the differences were statistically significant ($P<0.05$). The results were shown as Fig. 4 – 5.

3.3 Effect of Tianxiang Dan on autophagy and AIM2 inflammasome signaling pathway HE staining of mice in TXD group showed incomplete aortic intima, disordered arrangement of endothelial cells, lipid deposition and plaque formation on the vessel wall. Masson staining showed that collagen fibers were distributed in various layers of the vascular wall, with clear morphology. Immunohistochemistry showed a light brownish yellow positive

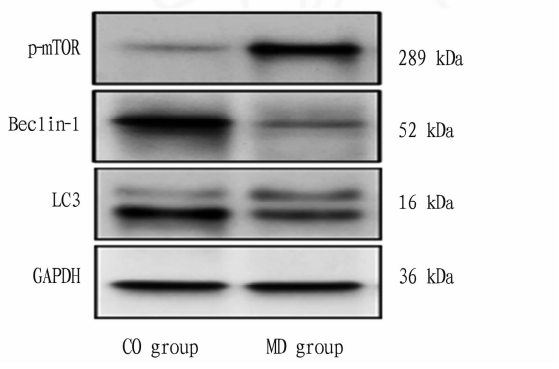
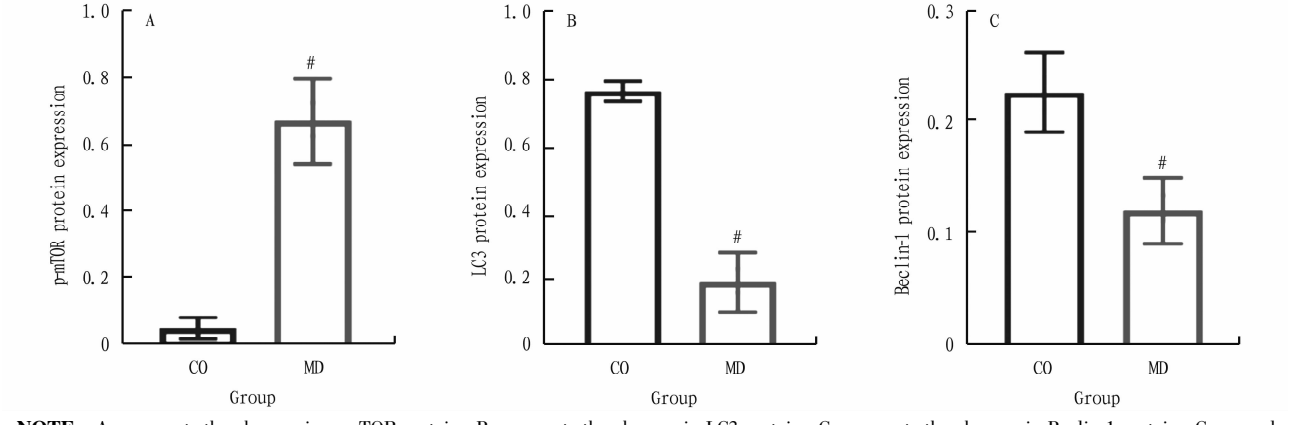


Fig. 4 Band diagram of autophagy pathway related protein expression in aortic tissues of two groups of mouse



NOTE A represents the changes in p-mTOR protein; B represents the changes in LC3 protein; C represents the changes in Beclin-1 protein. Compared with the CO group, # shows $P<0.05$.

Fig. 5 Comparison of protein expression related to autophagy pathway in aortic tissues of two groups of mouse

staining. HE staining of mice in NLRP3$^{-/-}$ group showed incomplete structure of the aortic intima, disordered arrangement of endothelial cells, lipid deposition and plaque formation on the vessel wall. Masson staining showed that collagen fibers were deposited on the vascular wall and arranged in disorder. Immunohistochemistry showed a light brownish yellow positive staining. HE staining of mice in RGFP966 group showed that the structure of the aortic intima was intact, the arrangement of endothelial cells was relatively regular, and there was no lipid deposition or plaque formation on the vascular wall. Masson staining showed the distribution of collagen fibers within the vascular wall, with a clear structure. The results were shown as Fig. 6. Compared with the MD group, the TXD group showed a decrease in the expression levels of AIM2, p-mTOR, Caspase-1, GSDMD, IL-1β, and IL-18 proteins, an increase in the expression levels of LC3 and Beclin-1 proteins, a decrease in serum IL-1β, IL-18 levels, and AIM2 mRNA expression level, with statistically significant differences ($P < 0.05$). Compared with the TXD group, the NLRP3$^{-/-}$ group showed an increase in the expression levels of AIM2, p-mTOR, Caspase-1, GSDMD proteins, and AIM2 mRNA, while the expression levels of IL-18, LC3, Beclin-1 protein, and serum IL-18 content decreased. The differences were statistically significant ($P < 0.05$). Compared with the TXD group, the RGFP966 group showed a significant decrease in IL-18 protein expression and serum IL-18 level ($P < 0.05$). The results were shown as Fig. 7 – 8.

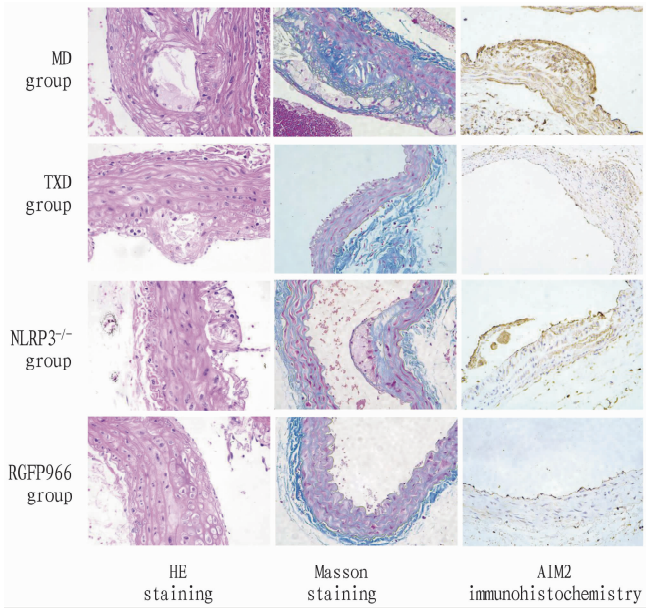
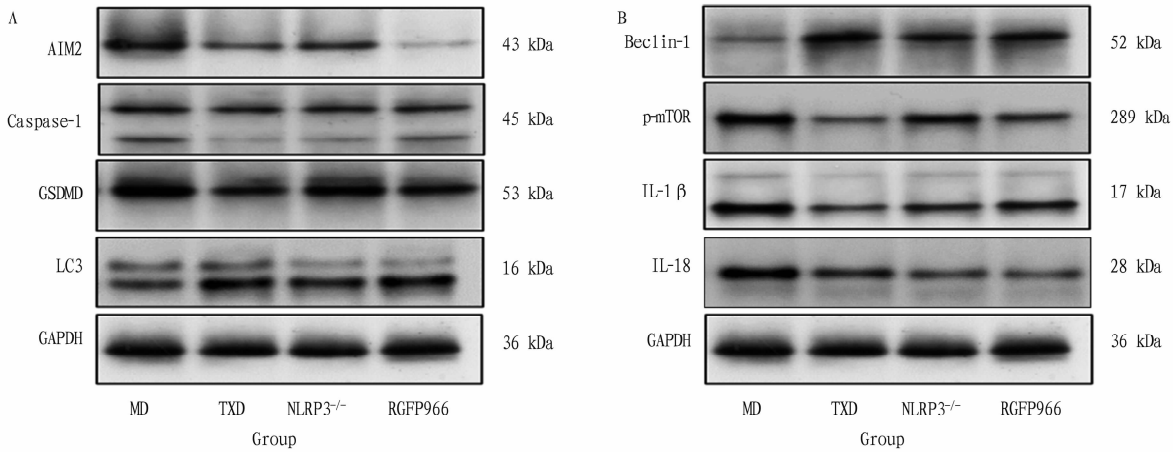


Fig. 6 Pathological changes in aortic tissue of mice in each group (×400)



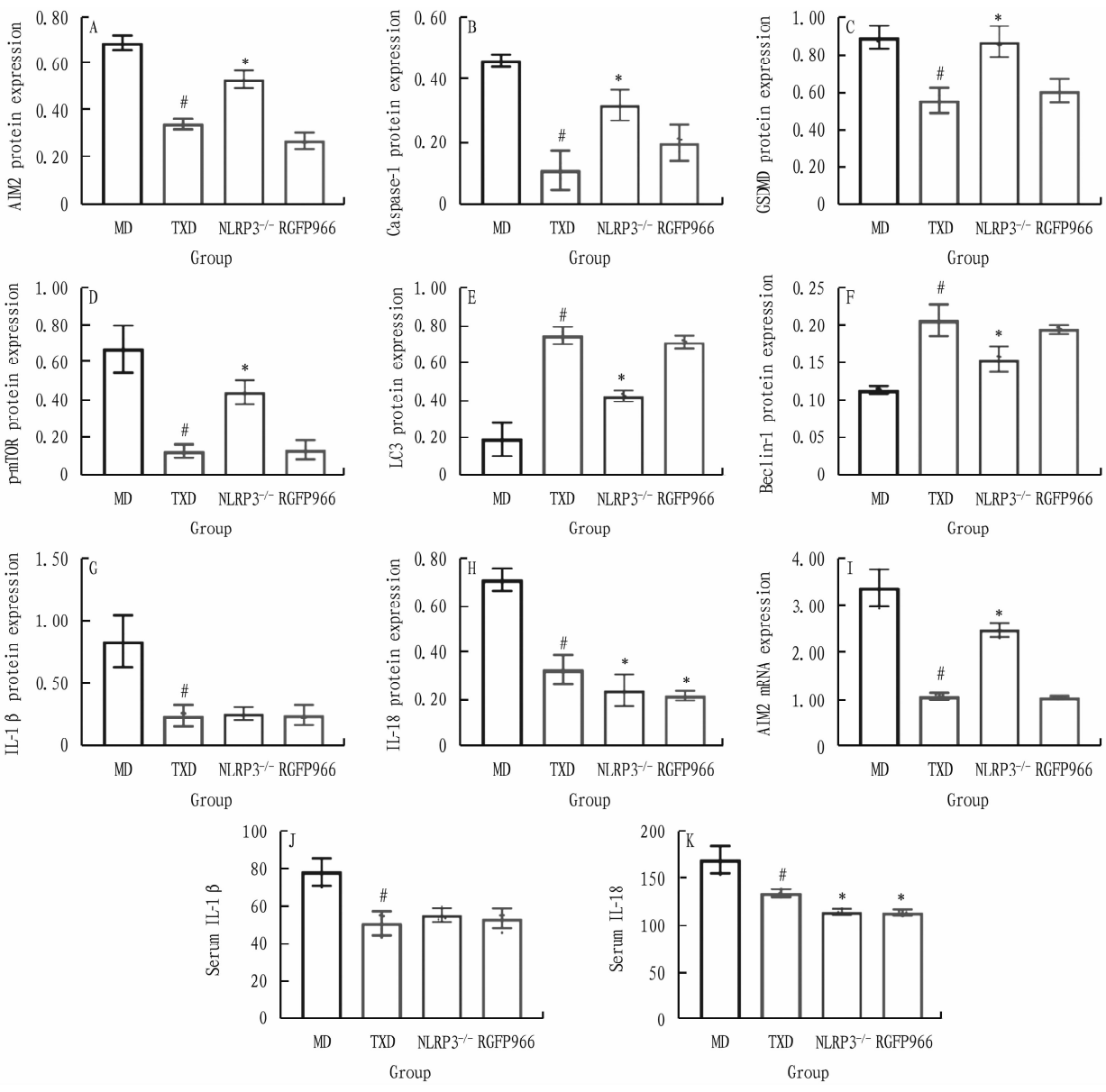
NOTE A is the expression band diagram of AIM2, Caspase-1, GSDMD, and LC3 proteins; B is the expression band diagram of Beclin-1, p-mTOR, IL-1β, and IL-18 proteins.

Fig. 7 Band diagram of protein expression related to aortic tissue in each group of mice

3.4 Tianxiang Dan improving AS by activating autophagy, inhibiting mTOR and AIM2 inflammasome Correlation analysis showed that LC3 was negatively correlated with AIM2, GSDMD, IL-1β and IL-18, and p-mTOR was positively correlated with AIM2, GSDMD, IL-1β and IL-18. It showed that Tianxiang Dan and RGFP966 might negatively regulate the activation of AIM2 inflammasome by regulating autophagy-mTOR pathway, thereby alleviating atherosclerosis. The results were shown as Fig. 9.

4 Discussion

Based on ApoE$^{-/-}$ and NLRP3$^{-/-}$ mouse atherosclerosis models, this paper observed the role of AIM2 inflammasome related signaling pathway in plaque formation, and revealed that RGFP966 negatively regulated AIM2 inflammasome and related signaling pathway through autophagy-mTOR pathway, thereby reducing the burden of atherosclerosis and vascular wall inflammation. It was found that autophagy inhibition, mTOR overactivation, AIM2 inflammasome activation, and enhanced cell pyroptosis coexisted in ApoE$^{-/-}$ mice; RGFP966 can restore autophagy, inhibit p-mTOR, and downregulate AIM2 and GSDMD activation; in the absence of NLRP3, AIM2 related changes and some effects of RGFP966 still existed, suggesting that AIM2 had an independent role

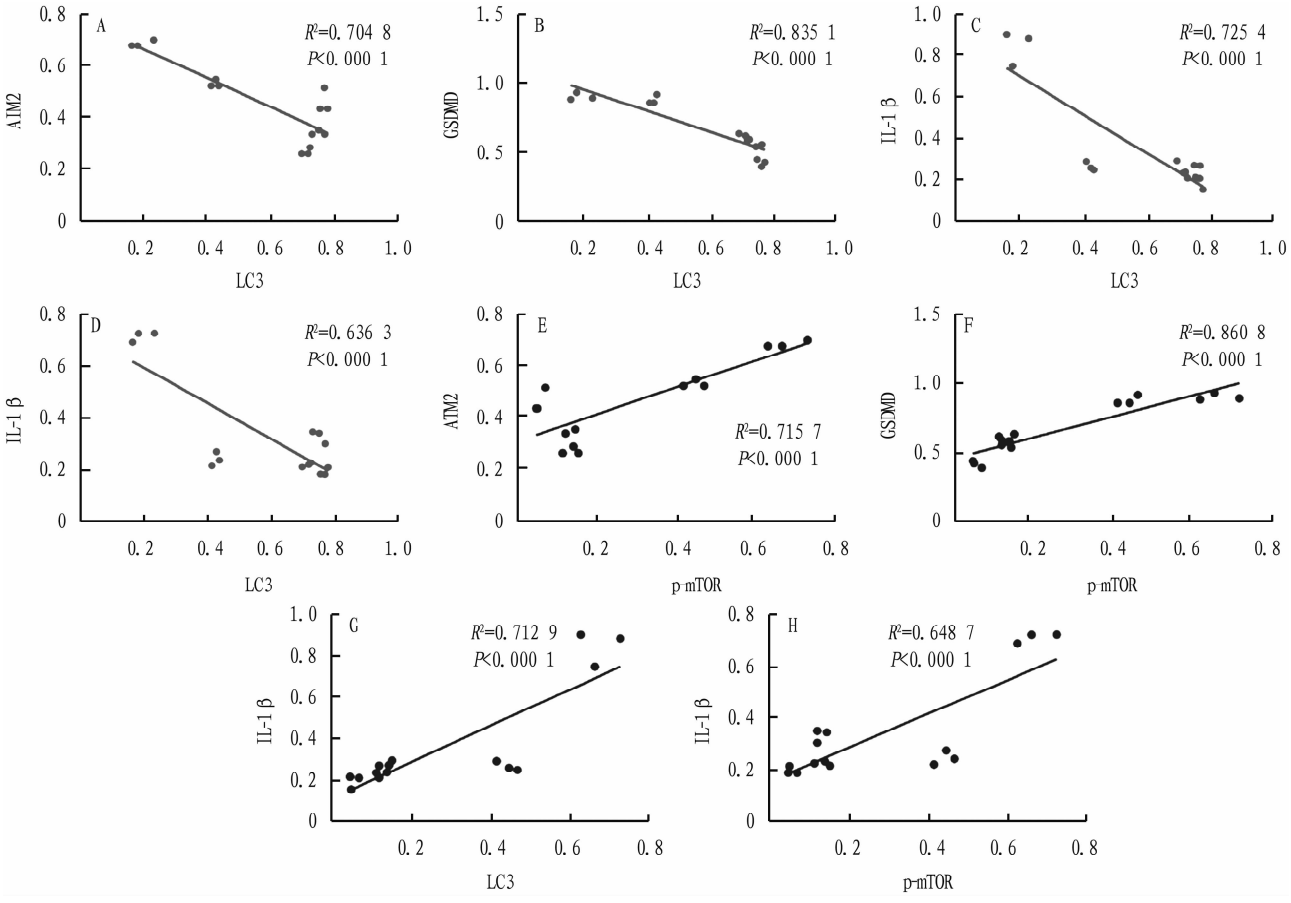


NOTE A represents the changes in AIM2 protein; B represents the changes in Caspase-1 protein; C represents the changes in GSDMD protein; D represents the changes in p-mTOR protein; E represents the changes in LC3 protein; F represents the changes in Beclin-1 protein; G represents the changes in IL-1β protein; H represents the changes in IL-18 protein; I represents the changes in AIM2 mRNA; J represents the changes in serum IL-1β; K represents the changes in serum IL-18. In the comparison between TXD group and MD group, # shows $P<0.05$; compared with the TXD group, * shows $P<0.05$.

Fig. 8 Comparison of protein and mRNA expression in aortic tissue and serum levels of IL-1β and IL-18 among different groups of mice

in atherosclerosis. Tianxiang Dan can slow down the progress of atherosclerosis by inhibiting the activation of AIM2 inflammasome and the recovery of autophagy pathway. Combined with previous studies[14-15], it confirmed the potential application value of Tianxiang Dan in this disease model.

This paper showed that the area of aortic plaque in TXD group mice was reduced, the thickness of fibrous cap was significantly increased, and the area of necrotic core was reduced, showing that Tianxiang Dan had a significant improvement effect on the pathological progression of atherosclerosis. Further analysis showed that the expression of AIM2 protein, Caspase-1, GSDMD levels, and inflammatory factors IL-1β and IL-18 were reduced in the aorta of TXD group mice. The above results indicated that Tianxiang Dan can effectively inhibit the activation of AIM2 inflammasome, and alleviate the cell pyroptosis reaction mediated by AIM2, thereby reducing inflammation and damage to the vascular wall. Tianxiang Dan had potential in the treatment of atherosclerosis. It can improve the stability of plaque by regulating the activation of AIM2 inflammasome.



NOTE A represents AIM2 and LC3; B represents GSDMD and LC3; C represents IL-1β and LC3; D represents IL-18 and LC3; E represents AIM2 and p-mTOR; F represents GSDMD and p-mTOR; G represents IL-1β and p-mTOR; H represents IL-18 and p-mTOR.

Fig. 9 Correlation analysis between AIM2, GSDMD, IL-1β, IL-18 and p-mTOR, LC3

This paper found that inhibition of autophagy and excessive activation of mTOR were accompanied by activation of AIM2 inflammasome in ApoE$^{-/-}$ mice, consistent with previous research results[16-17]. Autophagy defects often lead to accumulation of intracellular DNA and mitochondrial dysfunction, thereby promoting activation of AIM2 inflammasome. After intervention with Tianxiang Dan, autophagy activity was restored, and LC3 and Beclin-1 increased, indicating that Tianxiang Dan can restore autophagy function, which was consistent with previous research results[18]. This paper showed that Tianxiang Dan can inhibit the excessive activation of mTOR signaling and reduce the activation levels of AIM2 and its downstream GSDMD, Caspase-1, IL-1β, and IL-18. By regulating the autophagy-mTOR pathway, inhibiting the activation of AIM2 inflammasome, and reducing inflammatory reaction, Tianxiang Dan could improve atherosclerosis.

The results of this study also showed that RGFP966 increased autophagic activity, elevated LC3 and Beclin-1, and inhibited excessive activation of mTOR signaling. RGFP966 reduced the activation of AIM2 inflammasome by restoring autophagy and inhibiting mTOR activity, thereby decreasing the activation levels of AIM2, GSDMD, Caspase-1, IL-1β, and IL-18. This result showed that Tianxiang Dan can regulate the activation of AIM2 inflammasome through autophagy-mTOR pathway, thereby reducing the pathological damage of atherosclerosis, which may become an effective intervention strategy.

In the TXD group mice of this study, a high-fat diet can induce plaque formation to a certain extent, accompanied by upregulation of AIM2 protein expression and increased levels of IL-1β and IL-18, although NLRP3 related signals were significantly weakened. Further experiments showed that even in the absence of NLRP3, the activation of AIM2 inflammasome existed, indicating that AIM2 played an independent role in the progression of atherosclerosis. The intervention of Tianxiang Dan and RGFP966 can significantly inhibit the activation of AIM2 inflammasome, further confirming the pathogenic role of AIM2 as an independent inflammasome in atherosclerosis.

Limitations of this paper: firstly, this study was limited to a mouse model and lacked validation of human derived plaque tissue. Although the mouse model provides experimental data for the study of atherosclerosis, its differences with humans still need to be further explored. Secondly, the role of AIM2 in different cell types, including endothelial cells, smooth muscle cells, and macrophages, has not been finely analyzed at the cellular level. In the future, the specific effects of AIM2 on different cell types will be further explored through cell specific knockout mice or cell lines. Finally, although RGFP966 has significant effects on autophagy

and mTOR signaling pathways, its epigenetic regulatory targets and upstream signaling pathways have not been thoroughly elucidated. Future research should focus on the validation of human specimens, cell specific targeting, and precise localization of epigenetic targets, in order to provide theoretical basis for clinical applications.

In conclusion, inhibition of autophagy flow and over activation of mTOR were closely related to abnormal activation of AIM2 inflammasome and related signal pathways in ApoE$^{-/-}$ atherosclerosis model. The inhibitor RGFP966 significantly reduced AIM2 inflammasome activation and cell pyroptosis by restoring autophagy and inhibiting mTOR activity, reducing plaque burden and improving plaque stability. Tianxiang Dan can further slow down the progression of atherosclerosis by regulating autophagy and inhibiting the activation of AIM2 inflammasome, which confirmed its potential clinical application value. Autophagy-mTOR-AIM2 inflammasome provided a new therapeutic target for the prevention and treatment of atherosclerosis, and laid a foundation for the research of related intervention strategies.

References

[1] DUEWELL P, KONO H, RAYNER KJ, *et al.* NLRP3 inflammasomes are required for atherogenesis and activated by cholesterol crystals[J]. Nature, 2010, 464(7293): 1357 – 1361.

[2] TOLDO S, MEZZAROMA E, BUCKLEY LF, *et al.* Targeting the NLRP3 inflammasome in cardiovascular diseases[J]. Pharmacology & Therapeutics, 2022, 236: 108053.

[3] ZHENG YD, XU L, DONG NG, *et al.* NLRP3 inflammasome: The rising star in cardiovascular diseases[J]. Frontiers in Cardiovascular Medicine, 2022, 9: 927061.

[4] WORTMANN M, PETERS AS, ERHART P, *et al.* Inflammasomes in the pathophysiology of aortic disease[J]. Cells, 2021, 10(9): 2433.

[5] RüHL S, SHKARINA K, DEMARCO B, *et al.* ESCRT-dependent membrane repair negatively regulates pyroptosis downstream of GSDMD activation[J]. Science, 2018, 362(6417): 956 – 960.

[6] YIN Y, LI XY, SHA XJ, *et al.* Early hyperlipidemia promotes endothelial activation via a caspase-1-sirtuin 1 pathway[J]. Arteriosclerosis, Thrombosis, and Vascular Biology, 2015, 35(4): 804 – 816.

[7] ZHONG ZY, UMEMURA A, SANCHEZ-LOPEZ E, *et al.* NF-κB restricts inflammasome activation via elimination of damaged mitochondria[J]. Cell, 2016, 164(5): 896 – 910.

[8] DU LP, WANG XY, CHEN SY, *et al.* The AIM2 inflammasome: A novel biomarker and target in cardiovascular disease[J]. Pharmacological Research, 2022, 186: 106533.

[9] LIN L, ZHANG MX, ZHANG L, *et al.* Autophagy, pyroptosis, and ferroptosis: New regulatory mechanisms for atherosclerosis[J]. Frontiers in Cell and Developmental Biology, 2022, 9: 809955.

[10] KURDI A, MARTINET W, DE MEYER GRY. mTOR inhibition and cardiovascular diseases: Dyslipidemia and atherosclerosis[J]. Transplantation, 2018, 102(2S Suppl 1): S44 – S46.

[11] ZHANG SY, NIE FQ, ZENG YJ, *et al.* RGFP966 inhibits palmitic acid induced VSMCs phenotypic transition by targeting ATGL[J]. Biochimica et Biophysica Acta (BBA)-Molecular and Cell Biology of Lipids, 2025, 1870(3): 159597.

[12] HU Q, LI CY, ZHANG T, *et al.* Dihydromyricetin suppresses endothelial NLRP3 inflammasome activation and attenuates atherogenesis by promoting mitophagy[J]. Lipids in Health and Disease, 2024, 23(1): 279.

[13] GONG M, ZHU LL, CUI BD, *et al.* The active metabolites of *Eucommia ulmoides* leaves alleviate atherosclerosis induced by a high-fat diet and VD3 in rats[J]. Frontiers in Pharmacology, 2025, 16: 1625200.

[14] ZHENG XY, LUO ZH, ZHENG JL, *et al.* Electroacupuncture attenuates high-fat diet-exacerbated Alzheimer's pathology by enhancing TFEB/TFE3-mediated autophagic clearance of tau and NLRP3 inflammasome in 3xTg mice[J]. CNS Neuroscience & Therapeutics, 2025, 31(7): e70497.

[15] ZHAO MF, SUN LF, XIE XL, *et al.* Proteomic study of Tianxiangdan intervention in rats with myocardial ischemia[J]. Journal of Physiology and Pharmacology, 2022, 73(2). DOI: 10.26402/jpp.2022.2.13.

[16] FIDLER TP, XUE CY, YALCINKAYA M, *et al.* The AIM2 inflammasome exacerbates atherosclerosis in clonal haematopoiesis[J]. Nature, 2021, 592(7853): 296 – 301.

[17] SAWUER G, MA XK, ZHANG YJ, *et al.* Tianxiangdan improves coronary microvascular dysfunction in rats by inhibiting microvascular inflammation via Nrf2 activation[J]. Evidence-Based Complementary and Alternative Medicine, 2021, 2021: 4114784.

[18] MA XY, ZHAO HR, QIAO HL, *et al.* Mechanism of total flavonoids of *Ziziphora clinopodioides* in improving atherosclerosis by regulating PI3K/Akt/mTOR pathway[J]. China Journal of Chinese Materia Medica, 2023, 48(2): 465 – 471. (in Chinese).

Medicinal Plant (ISSN 2152 – 3924), founded by Wu Chu (USA – China) Science and Culture Media Corporation in 2010, is a bimonthly medicinal academic journal published and approved by the Library of Congress of the United States of America. Papers in *Medicinal Plant* cover the quality control of Chinese medicine processing, analysis of chemical components of medicinal plants and extraction of active composition, pharmacology and toxicology, biotechnology, clinical applications, germplasm resources and cultivation.

Medicinal Plant is indexed by the following databases:

▶CNKI (China National Knowledge Infrastructure), China
▶SuperStar Digital Library (China)
▶Chongqing VIP Information Co., Ltd.
▶Chemical Abstracts (CA), USA
▶Center for Agriculture and Biosciences International (CABI), UK
▶EBSCO, USA
▶CSA Illumina (Cambridge Scientific Abstracts), USA
▶AGRIS, FAO
▶KIT Royal Tropical Institute (Amsterdam, the Netherlands)
▶Rural Development Foundation (RDF), India